Proceedings of the
International Conference on Mechanical Engineering 2011
(ICME2011) 18-20 December 2011, Dhaka, Bangladesh

ICME11-TH-044

EFFECT OF DIMENSIONLESS NUMBER ON NATURAL CONVECTION IN AN OPEN SQUARE CAVITY HAVING PARTIALLY HEATED SQUARE CYLINDER

Mohammed Nasir Uddin[1] and Mohammad Abdul Alim[2]

[1]Department of Mathematics, Bangladesh University of Business & Technology (BUBT), Dhaka, Bangladesh
[2]Department of Mathematics, Bangladesh University of Engineering & Technology (BUET), Dhaka, Bangladesh

ABSTRACT

A numerical analysis of two-dimensional laminar steady-state natural convection in a square tilted open cavity (SOC) having partially heated square cylinder has been numerically studied. The opposite wall to the aperture is placed at iso-flux heat source q, while the surrounding fluid interacting with the aperture is maintained at an ambient temperature T_∞. The other two remaining walls were kept cooled Temperature T_c (Top wall) and heated temperature T_h (bottom wall). The fluid concerned with different Prandtl number (Pr) at 0.72, 1 and 7. The governing mass, momentum and energy equations are expressed in a normalized primitive variables formulation. In this paper, the effect of dimensionless number for steady-state incompressible natural convection flows has been developed. The streamlines and isotherms are produced. The heat transfer characteristics is obtained for Grashof numbers (Gr) from 10^3 to 10^6 , for an inclination angles of the cavity ranges from 0º to 45º and different length ratio (*l*r) of cylinder. The results show that the Nusselt numbers (Nu) increases with the increases of Grashof numbers. Also the average Nusselt number (Nu_{av}) changes substantially with the inclination angle of the cavity while thermal performance is also sensitive to the boundary condition of the heated wall.

Keywords: Natural Convection, Finite Element Method, Grashof Number, Open Square Cavity, Partially Heated Square Cylinder.

1. INTRODUCTION

Natural convection (NC) in open cavities has received considerable attention because of its importance in several thermal engineering problems, for example, in the design of electronic devices, solar thermal receivers, uncovered flat plate solar collectors having rows of vertical strips geothermal reservoirs, etc. During the past two decades, several experiments and numerical calculations have been presented for describing the phenomenon of NC in open cavities. Those studies have been focused in the present work to study the effect on flow and heat transfer for different Gr, aspect ratios, and tilt angles. Le Quere et al. [7] investigated thermally driven laminar natural convection in enclosures with isothermal sides, one of which facing the opening using finite difference. Penot [5] studied a similar problem using stream function-vorticity formulation. Chan and Tien [2] studied numerically shallow open cavities and also made a comparison study using a square cavity in an enlarged computational domain. In similar way, Mohamad [4] studied inclined SOC, by considering a restricted computational domain. Polat and Bilgen [6] studied numerically inclined open shallow cavities in which the side facing the opening was heated by constant heat flux, two adjoining walls were insulated and the opening was in contact with a reservoir at constant temperature and pressure. The computational domain was restricted to the cavity. Angirasa [1] showed that the inclusion of the outside domain into the computations has a minimal effect on the heat transfer results for those cavities where one wall is isothermal and other two walls are adiabatic. Goutam saha et. al.[8] Studied that a square tilted SOC has an effect on the heat transfer results for those cavities where one wall is either isothermal heat source or iso-flux heat source and other two walls are adiabatic using FEM. As the first step toward accurate flow solutions using the adaptive meshing technique [3], this paper develops a finite element formulation suitable for analysis of steady-state NC flow problems. The paper starts from the Navier-Stokes equations together with the energy equation to derive the corresponding finite element equations. The computational procedure used in the development of the computer program is described. The finite element equations derived and then the computer program developed are then evaluated by example of natural convection in a square open cavity.

2. PHYSICAL MODEL AND ASSUMPTIONS

The heat transfer and the fluid flow in a two-dimensional open square cavity of length L having partially heated square cylinder with length ratio (*l*r) are considered, as shown in the schematic diagram of fig.-1. The opposite wall to the aperture is placed at iso-flux heat source q, while the surrounding fluid interacting with the aperture is maintained to an ambient temperature T_{∞}. The other two remaining walls were kept cooled Temperature T_c (Top wall) and heated temperature T_h (bottom wall). The fluid is assumed to be different prandtl number (Pr = 0.72, 1.0 & 7) and Newtonian, and the fluid flow is considered to be laminar. The properties of the fluid are assumed to be constant.

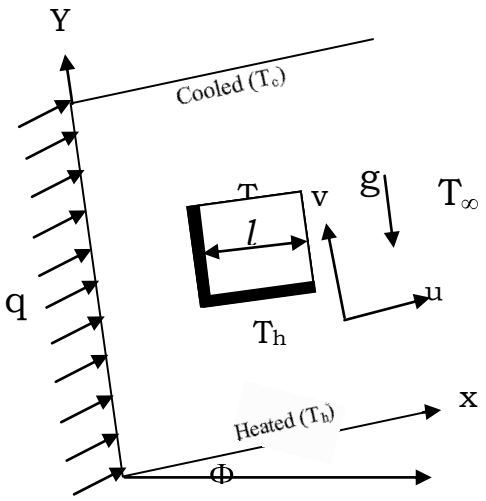

Fig 1. Schematic diagram of the square open cavity

3. MATHEMATICAL MODEL

Natural convection is governed by the differential equations expressing conservation of mass, momentum and energy. The present flow is considered steady, laminar, incompressible and two-dimensional. The viscous dissipation term in the energy equation is neglected. The Boussinesq approximation is invoked for the fluid properties to relate density changes to temperature changes, and to couple in this way the temperature field to the flow field. The governing equations in non-dimensional form are written as follow:

$$\frac{\partial U}{\partial X}+\frac{\partial V}{\partial Y}=0$$

with the boundary conditions

$$\frac{\partial \theta}{\partial Y}(X,0)=\frac{\partial \theta}{\partial Y}(X,1)=0\ \frac{\partial \theta}{\partial X}(0,Y)=-1$$

$$\frac{\partial U}{\partial X}(1,Y)=\frac{\partial V}{\partial X}(1,Y)=0\ \frac{\partial \theta}{\partial X}(1,Y)=0$$

θ (0,Y) = 1

The above equations were normalized using the following dimensionless scales:

$$X=\frac{x}{L}\ Y=\frac{y}{L}\ U=\frac{u}{U_0}\ V=\frac{v}{U_0}\ \mathrm{Pr}=\frac{\nu}{\alpha}$$

$$P=\frac{p-p_{\infty}}{\rho U_0^2}\quad \theta=\frac{T-T_{\infty}}{\Delta T}\ Gr=\frac{g\beta\Delta TL^3}{\nu^2}$$

$$\Delta T=\frac{qL}{k}\quad dr=\frac{D}{L}$$

The Nusselt number (Nu) is one of the important dimensionless parameters to be computed for heat transfer analysis in natural convection flow. The local Nusselt number can be obtained from the temperature field by applying Nu = – 1/ θ(0,Y) and the average or overall Nusselt number was calculated by integrating the temperature gradient over the heated wall as

$$Nu_{av}=-\int_0^1\frac{1}{\theta(0,Y)}dY$$

4. FINITE ELEMENT FORMULATION

The velocity and thermal energy equations result in a set of non-linear coupled equations for which an iterative scheme is adopted. To ensure convergence of the numerical algorithm the following criteria is applied to all dependent variables over the solution domain

$$\sum\left|\phi_{ij}^{m}-\phi_{ij}^{m-1}\right|\le 10^{-5}$$

where φ represents a dependent variable U, V, P, and T; the indexes i, j indicate a grid point; and the index m is the current iteration at the grid level. The six node triangular element is used in this work for the development of the finite element equations. All six nodes are associated with velocities as well as temperature; only the corner nodes are associated with pressure. This means that a lower order polynomial is chosen for pressure and which is satisfied through continuity equation. The velocity component and the temperature distributions and linear interpolation for the pressure distribution according to their highest derivative orders in the differential Equations as

$$U(X,Y)=N_{\alpha}U_{\alpha}$$
$$V(X,Y)=N_{\alpha}U_{\alpha}$$
$$\theta(X,Y)=N_{\alpha}\theta_{\alpha}$$
$$P(X,Y)=H_{\lambda}P_{\lambda}$$

where α = 1, 2, … …, 6; λ= 1, 2, 3; N_{α} are the element interpolation functions for the velocity components and the temperature, and H_{λ} are the element interpolation functions for the pressure.

To derive the finite element equations, the method of

weighted residuals is applied to the continuity Equation. the momentum Equations and the energy Equation, we get

$$\int_A N_\alpha (U\frac{\partial U}{\partial X}+\frac{\partial V}{\partial U})\,dA=0$$

$$\int_A N_\alpha\left(U\frac{\partial U}{\partial X}+V\frac{\partial U}{\partial Y}\right)\,dA=-\int_A H_\lambda\left(\frac{\partial P}{\partial X}\right)\,dA$$
$$+\frac{1}{\sqrt{Gr}}\int_A N_\alpha\left(\frac{\partial^2 U}{\partial X^2}+\frac{\partial^2 U}{\partial Y^2}\right)\,dA+\int_A N_\alpha(\sin\Phi)\theta dA$$

$$\int_A N_\alpha\left(U\frac{\partial V}{\partial X}+V\frac{\partial V}{\partial Y}\right)\,dA=-\int_A H_\lambda\left(\frac{\partial P}{\partial Y}\right)\,dA$$
$$+\frac{1}{\sqrt{Gr}}\int_A N_\alpha\left(\frac{\partial^2 V}{\partial X^2}+\frac{\partial^2 V}{\partial Y^2}\right)dA+\int_A N_\alpha(\cos\Phi)\theta dA$$

$$\int_A N_\alpha\left(U\frac{\partial\theta}{\partial X}+V\frac{\partial\theta}{\partial Y}\right)\,dA=\frac{1}{\Pr\sqrt{Gr}}\int_A N_\alpha\left(\frac{\partial^2\theta}{\partial X^2}+\frac{\partial^2\theta}{\partial Y^2}\right)\,dA$$

Where dA is the element area, Gauss's theorem is then applied to generate the boundary integral terms associated with the surface tractions and heat flux. Then Equations become,

$$\int_A N_\alpha\left(U\frac{\partial U}{\partial X}+V\frac{\partial U}{\partial Y}\right)\,dA+\int_A H_\lambda\left(\frac{\partial P}{\partial X}\right)\,dA+$$
$$\frac{1}{\sqrt{Gr}}\int_A\left(\frac{\partial N_\alpha}{\partial X}\frac{\partial U}{\partial X}+\frac{\partial N_\alpha}{\partial Y}\frac{\partial U}{\partial Y}\right)dA-\int_A\sin\Phi N_\alpha\theta dA=\int_{S_0}N_\alpha S_x dS_0$$

$$\int_A N_\alpha\left(U\frac{\partial V}{\partial X}+V\frac{\partial V}{\partial Y}\right)\,dA+\int_A H_\lambda\left(\frac{\partial P}{\partial Y}\right)dA+$$
$$\frac{1}{\sqrt{Gr}}\int_A\left(\frac{\partial N_\alpha}{\partial X}\frac{\partial V}{\partial X}+\frac{\partial N_\alpha}{\partial Y}\frac{\partial V}{\partial Y}\right)dA-\int_A\cos\Phi N_\alpha\theta dA=\int_{S_0}N_\alpha S_y dS_0$$

$$\int_A N_\alpha\left(U\frac{\partial\theta}{\partial X}+V\frac{\partial\theta}{\partial Y}\right)\,dA+\frac{1}{\Pr\sqrt{Gr}}\int_A\left(\frac{\partial N_\alpha}{\partial X}\frac{\partial\theta}{\partial X}+\frac{\partial N_\alpha}{\partial Y}\frac{\partial\theta}{\partial Y}\right)\,dA$$
$$=\int_{S_w}N_\alpha\;\;q_w\;\;dS_w$$

Here specifying surface tractions (S_x, S_y) along outflow boundary S_0 and specifying velocity components and fluid temperature or heat flux that flows into or out from domain along wall boundary S_w. Substituting the element velocity component distributions, the temperature distribution, and the pressure distribution from Equations, the finite element equations can be written in the form,

$$K_{\alpha\beta^x}U_\beta+K_{\alpha\beta^y}V_\beta=0$$

$$K_{\alpha\beta\gamma^x}U_\beta U_\gamma+K_{\alpha\beta\gamma^y}V_\gamma U_\gamma+M_{\alpha\mu^x}P_\mu+\frac{1}{\sqrt{Gr}}\;\;S_{\alpha\beta^{xx}}+S_{\alpha\beta^{yy}}\;\;U_\beta$$
$$-\;\;\sin\Phi\;\;K_{\alpha\beta}\theta_\beta=Q_{\alpha^u}$$

$$K_{\alpha\beta\gamma^x}U_\beta V_\gamma+K_{\alpha\beta\gamma^y}V_\gamma V_\gamma+M_{\alpha\mu^y}P_\mu+\frac{1}{\sqrt{Gr}}\;\;S_{\alpha\beta^{xx}}+S_{\alpha\beta^{yy}}\;\;V_\beta$$
$$-\;\;\cos\Phi\;\;K_{\alpha\beta}\theta_\beta=Q_{\alpha^v}$$

$$K_{\alpha\beta\gamma^x}U_\beta\theta_\gamma+K_{\alpha\beta\gamma^y}V_\beta\theta_\gamma+\frac{1}{\Pr\sqrt{Gr}}\;\;S_{\alpha\beta^{xx}}+S_{\alpha\beta^{yy}}\;\;\theta_\beta=Q_{\alpha^T}$$

where the coefficients in element matrices are in the form of the integrals over the element area and along the element edges S_0 and S_w as,

$$K_{\alpha\beta^x}=\int_A N_\alpha N_{\beta,x}dA$$
$$K_{\alpha\beta^y}=\int_A N_\alpha N_{\beta,y}dA$$
$$K_{\alpha\beta\gamma^x}=\int_A N_\alpha N_\beta N_{\gamma,x}dA$$
$$K_{\alpha\beta\gamma^y}=\int_A N_\alpha N_\beta N_{\gamma,y}dA$$
$$K_{\alpha\beta}=\int_A N_\alpha N_\beta dA$$
$$S_{\alpha\beta^{yy}}=\int_A N_{\alpha,y}N_{\beta,y}dA$$
$$M_{\alpha\mu^x}=\int_A H_\alpha H_{\mu,x}dA$$
$$M_{\alpha\mu^y}=\int_A H_\alpha H_{\mu,y}dA$$
$$Q_{\alpha^u}=\int_{S_0}N_\alpha S_x dS_0\;,\;Q_{\alpha^v}=\int_{S_0}N_\alpha S_y dS_0$$
$$Q_\alpha\theta=\int_{S_w}N_\alpha\;\;q_w dS_w$$

These element matrices are evaluated in closed-form ready for numerical simulation. Details of the derivation for these element matrices are omitted herein for brevity.

5. COMPUTATIONAL PROCEDURE

The derived finite element equations are nonlinear. These nonlinear algebraic equations are solved by applying the Newton-Raphson iteration technique [3] by first writing the unbalanced values from the set of the finite element Equations as,

$$F_{\alpha^p}=K_{\alpha\beta^x}U_\beta+K_{\alpha\beta^y}V_\beta$$
$$F_{\alpha^u}=K_{\alpha\beta\gamma^x}U_\beta U_\gamma+K_{\alpha\beta\gamma^y}V_\gamma U_\gamma+M_{\alpha\mu^x}P_\mu+$$
$$\frac{1}{\sqrt{Gr}}\;\;(S_{\alpha\beta^{xx}}+S_{\alpha\beta^{yy}})\;\;U_\beta-\;\;\sin\Phi\;\;K_{\alpha\beta}\theta_\beta-Q_{\alpha^u}$$
$$F_{\alpha^v}=K_{\alpha\beta\gamma^x}U_\beta V_\gamma+K_{\alpha\beta\gamma^y}V_\gamma V_\gamma+M_{\alpha\mu^y}P_\mu$$
$$+\frac{1}{\sqrt{Gr}}(S_{\alpha\beta^{xx}}+S_{\alpha\beta^{yy}})V_\beta-\cos\Phi\;\;K_{\alpha\beta}\theta_\beta-Q_{\alpha^v}$$
$$F_{\alpha^T}=K_{\alpha\beta\gamma^x}U_\beta\theta_\gamma+K_{\alpha\beta\gamma^y}V_\beta\theta_\gamma+$$
$$\frac{1}{\Pr\sqrt{Gr}}\;\;S_{\alpha\beta^{xx}}+S_{\alpha\beta^{yy}}\;\;\;\;\theta_\beta-Q_{\alpha^T}$$

This leads to a set of algebraic equations with the incremental unknowns of the element nodal velocity components, temperatures, and pressures in the form,

$$\begin{bmatrix}K_{uu}&K_{uv}&K_{u\theta}&K_{up}\\K_{vu}&K_{vv}&K_{v\theta}&K_{vp}\\K_{Tu}&K_{\theta v}&K_{\theta\theta}&0\\K_{pu}&K_{pv}&0&0\end{bmatrix}\begin{Bmatrix}\Delta u\\\Delta v\\\Delta\theta\\\Delta p\end{Bmatrix}=-\begin{Bmatrix}F_{\alpha^u}\\F_{\alpha^v}\\F_{\alpha^\theta}\\F_{\beta^p}\end{Bmatrix}$$

Where,

$$K_{uu} = K_{\alpha\beta\gamma^x} U_\gamma + K_{\alpha\gamma\beta^x} U_\gamma + K_{\alpha\beta\gamma^y} V_\beta + \frac{1}{\sqrt{Gr}} \left(S_{\alpha\beta^{xx}} + S_{\alpha\beta^{yy}} \right)$$

$$K_{uv} = K_{\alpha\beta\gamma^y} U_\gamma ,$$

$$K_{u\theta} = -\sin\Phi \; K_{\alpha\beta}$$

$$K_{up} = M_{\alpha\mu^x} ,$$

$$K_{vu} = K_{\alpha\beta\gamma^x} V_\gamma$$

$$K_{vv} = K_{\alpha\beta\gamma^x} U_\beta + K_{\alpha\gamma\beta^y} V_\gamma + K_{\alpha\beta\gamma^y} V_\gamma + \frac{1}{\sqrt{Gr}} \left(S_{\alpha\beta^{xx}} + S_{\alpha\beta^{yy}} \right)$$

$$K_{v\theta} = -\cos\Phi \; K_{\alpha\beta} ,$$

$$K_{vp} = M_{\alpha\mu^y}$$

$$K_{\theta v} = K_{\alpha\beta\gamma^y} \theta\gamma ,$$

$$K_{p\theta} = 0 = K_{pp}$$

$$K_{\theta\theta} = K_{\alpha\beta\gamma^x} U_\beta + K_{\alpha\beta\gamma^y} V_\beta + \frac{1}{\Pr\sqrt{Gr}} S_{\alpha\beta^{xx}} + S_{\alpha\beta^{yy}}$$

$$K_{\theta p} = 0 \; K_{pu} = K_{\alpha\beta^x}$$

$$K_{pv} = K_{\alpha\beta^y}$$

The iteration process is terminated if the percentage of the overall change compared to the previous iteration is less than the specified value.

6. RESULTS AND DISCUSSION

The present problem is a square open cavity with the left vertical wall is at iso-flux heat source, while the top and bottom walls are cooled and heated temperature respectively. Obviously for high values of Grashof number the errors encountered are appreciable and hence it is necessary to perform some grid size testing in order to establish a suitable grid size. Grid independent solution is ensured by comparing the results of different grid meshes for Gr = 10^6, which was the highest Grashof number. The total domain is discretized into 13948 elements that results in 83688 nodes. In order to validate the numerical code, pure natural convection with Pr = 0.72 in a square open cavity was solved and the average Nusselt numbers is presented in graphically. The results were compared with those reported by Hinojosa et al. obtained with an extended computational domain. In Table-1, a comparison between the average Nusselt numbers is presented. The results from the present experiment are almost same as Hinojosa et al.

Table 1: Comparison of the results for the constant surface temperature with Pr = 0.71.

Ra	Nu_{av}	
	Present work	Hinojosa et al. (2005)
10^3	1.33	1.30
10^4	3.42	3.44
10^5	7.40	7.44
10^6	14.41	14.51

The effect of inclination angle is examined for Φ = 0º, 15º, 30º & 45º and with aspect ratio A = 1. The hydrodynamic and thermal field in the cavity in the form of streamlines and isotherms for different Grashof numbers are shown in Figures 2 to 7 for different angles, different lr and different Pr as representative cases. A steady-state pattern of streamlines from Gr of 10^3 to 10^6 with different angles is presented in Figure 2. Also the steady-state patterns of isotherms from Gr of 10^3 to 10^6 with different angles are presented in Figure 3. The streamlines and isotherms are shown for different lr and Pr in Figure 4 to 7. For the isotherm, the figures show that as the Gr and the inclination angle increases, the buoyancy force increases and the thermal boundary layers become thinner. For the streamlines, the figures show that the fluid enters from the bottom of the aperture, circulates in a clockwise direction following the shape of the cavity, and leaves toward the upper part of the aperture. The streamline patterns is very similar for last one Gr and the inclination angles, but the fluid moves faster and created vortices for Gr of 10^3 to 10^5, the streamline patterns is similar but the upper boundary layer becomes thinner and faster, the velocity of the air flow moving toward the aperture increases, and the area that is occupied by the leaving hot fluid decreases compared with that of the entering fluid.

Therefore, we see that as Gr increases, the flow gradually becomes convective dominated, the cold fluid is entrained right to the left vertical wall where high temperature gradients are created, and the discharging fluid from the upper part of the cavity occupies smaller section of the opening. Isotherms and streamlines show that as the inclination angle of the heated wall increases, the velocity gradient increases at heated wall, the strength of the circulation increases. The variation of the average Nusselt number with the Grashof number for the iso-flux heat source and lr is shown in Figures 8,9,10 and 11.Where Nu_{av} increases with increasing of Gr and increasing of lr. The heat transfer characteristics become lower for lower lr = 0.2 and higher for higher for lr = 0.4. At angle 0^0, The NU_{av} variation for different Prandtl numbers while Pr= 0.72, 1 & 7 in figure 10 shown that average Nusselt number (Nu_{av}) increases with increasing of Gr and increasing of Pr. At angle 30^0, the average Nusselt number (Nu_{av}) increases with increasing of Gr but decreasing of Pr which is shown in figure-11.The heat transfer characteristics become high for lower Pr = 0.72 and low for higher for Pr = 7.

Gr =10^3 Gr=10^5 Gr = 10^6

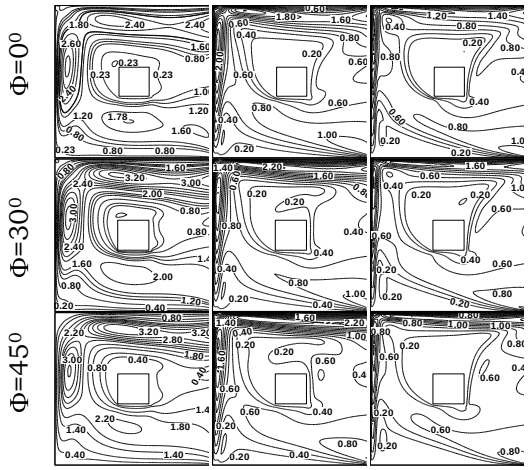

Figure-2: stream lines with different Gr and inclination angles when Pr = 0.72

Gr=10^3 Gr=10^5 Gr = 10^6

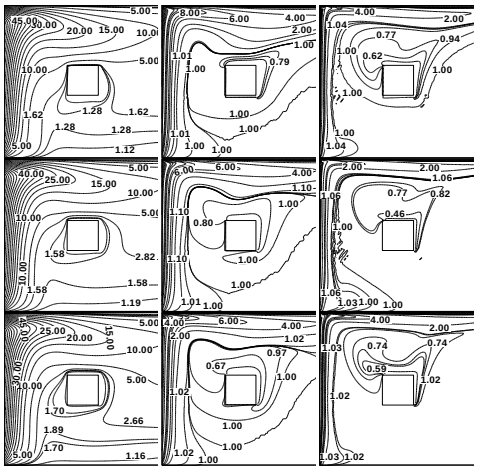

Figure-3: Isotherm lines with different Gr and inclination angles when Pr = 0.72

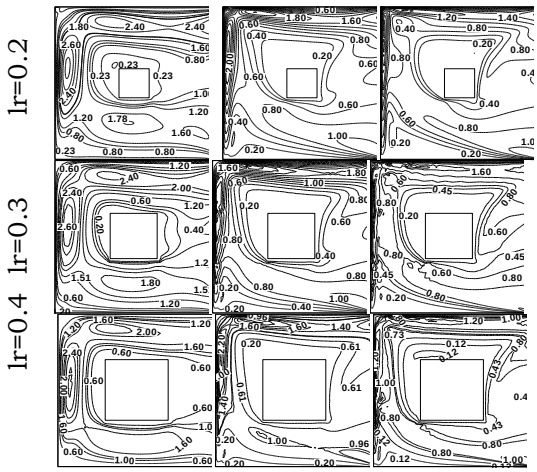

Figure-4: Stream lines with different Gr& lr with angles 0^0 when Pr = 0.72

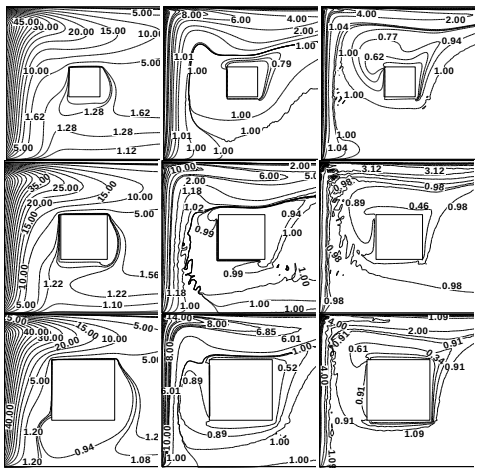

Figure-5: Isotherm lines with different Gr& lr with angles 0^0 when Pr = 0.72

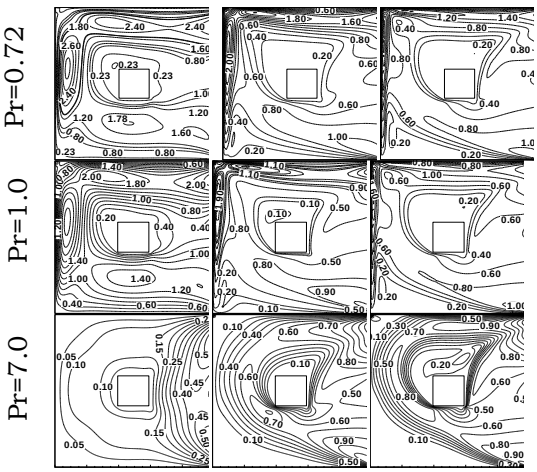

Figure-6: Stream lines with different Gr & Pr with angles 0^0

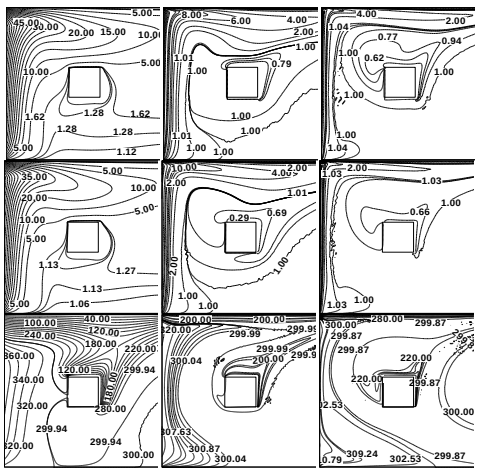

Figure-7: Stream lines with different Gr & Pr with angles 0^0

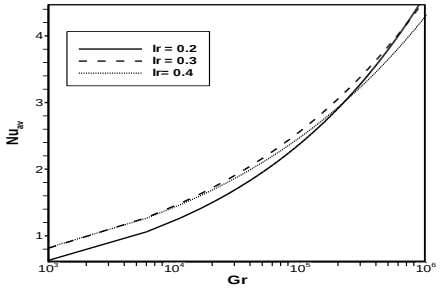

Fig 8: Variation of the Nu_{av} with the Gr for different lr.

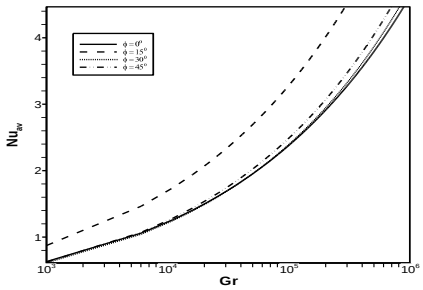

Fig 9. Variation of the Nu_{av} with the Gr for different angles.

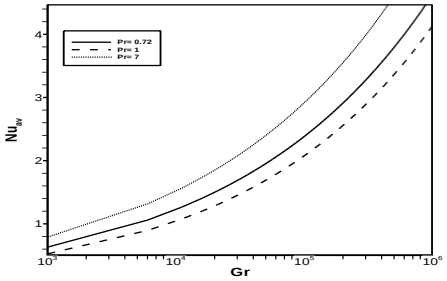

Fig 10: Variation of the Nu_{av} with the Gr for different Pr at 0^0.

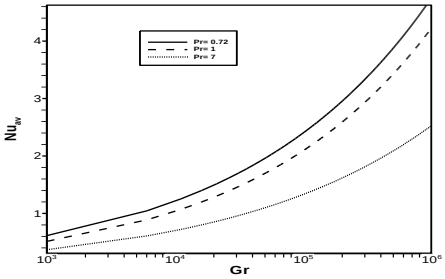

Fig 11. Variation of the Nu_{av} with the Gr for different Pr at 30^0

7. CONCLUSION

A finite element method for steady-state incompressible natural convection flow is presented. The finite element equations were derived from the governing flow equations that consist of the conservation of mass, momentum, and energy equations. The derived finite element equations are nonlinear requiring an iterative technique solver. The Galerkin weighted residual method is applied to solve these nonlinear equations for solutions of the nodal velocity components, temperatures, and pressures. The above example demonstrates the capability of the finite element formulation that can provide insight to steady-state incompressible natural convection flow behaviors.

8. REFERENCES

[1] Angirasa, D., Pourquie, M. J., and Nieuwstadt, F. T., 1992, "Numerical study of transient and steady laminar buoyancy-driven flows and heat transfer in a square open cavity", Numerical Heat Transfer, 22: 223-239.

[2] Chan, Y. L. and Tien, C. L., 1985, "A Numerical study of two-dimensional laminar natural convection in a shallow open cavity", Int. J. Heat Mass Transfer, 28: 603-612.

[3] Dechaumphai, P., 1995, "Adaptive finite element technique for heat transfer problems", Heat & Mass transfer, 17: 87-94.

[4] Mohamad, A., 1995, "Natural convection in open cavities and slots", Numerical Heat Transfer A, 27: 705-716.

[5] Penot, F., 1982, "Numerical calculation of two-dimensional natural convection in isothermal open cavities", Numerical Heat Transfer, 5: 421-437.

[6] Polat, O. and Bilgen, E., 2002, "Laminar natural convection in inclined open shallow cavities", Int. J. Therm Sci, 41: 360-368.

[7] Quere, P. Le, Humphery, J. A., and Sherman, F.S., 1981, "Numerical calculation of thermally driven two-dimensional unsteady laminar flow in cavities of rectangular cross section", Numerical Heat Transfer, 4: 249-283.

[8] Saha G., 2007, "A finite element method for steady state natural convection in a square tilt ope cavity", ARPN Journal of Engineering and Applied Sciences, 2:41-49.

9. NOMENCLATURE

Symbol	Meaning	Unit
g	gravitational acceleration	(ms–2)
k	thermal conductivity of the fluid	(m^3/s)
L	hight and width of the enclosure	–
P	pressure	–
P	non-dimensional pressure	–
q	heat flux	–
Nu	Nusselt number	
Pr	Prandtl number	–
T	Temperature	(K)
θ	dimensional temperature	(ms^{-1})
U,V	non-dimensional Velocity component	(ms^{-1})
Gr	Grashof number	–
u,v	velocity components	–
x,y	Cartesian coordinates	(m)
X,Y	non-dimensional Cartesian coordinates	(m)
α	thermal diffusivity	–
ρ	density of the fluid	–